Ecological Engineering 158 (2020) 106033

Contents lists available at ScienceDirect

Ecological Engineering

journal homepage: www.elsevier.com/locate/ecoleng

Soil carbon–nitrogen coupled accumulation following the natural vegetation restoration of abandoned farmlands in a karst rocky desertification region

Jiacheng Lan[a], Ning Hu[b,c,*], Wali Fu[c]

[a] School of Karst Science/State Engineering Technology Institute for Karst Desertification control, Guizhou Normal University, Guiyang 550001, People's Republic of China
[b] Earthquake Agency of Xinxiang City, Xinxiang 453000, People's Republic of China
[c] School of Geographical Sciences, Southwest University, Chongqing 400715, People's Republic of China

A R T I C L E I N F O

Keywords:
Vegetation restoration
Carbon–nitrogen accumulation
Soil N transformation
Soil N availability
Karst region

A B S T R A C T

Vegetation restoration on abandoned farmlands is one of the typical methods for accumulating soil organic carbon (OC) and total nitrogen (TN). However, the coupling of soil OC and N accumulation following vegetation restoration remain poorly known in karst rocky desertification regions in Southwest China. Four natural vegetation restoration lands, namely, grassland, shrubland, secondary forest I, and secondary forest II, were chosen with farmland as a reference. Soil samples were collected to determine the soil aggregates, soil OC and TN accumulation, soil inorganic N content, and soil N transformation rates. The amount of different soil aggregates fractions and stability of soil aggregates, levels of soil OC and TN in whole soil and aggregates, levels of soil inorganic N, and soil N transformation rates were considerably increased by vegetation restoration following farmland abandonment. The increases in total soil OC and TN stocks mainly contributed to the increase of OC and TN stocks in large aggregates. The soil C:N ratios and amount of exchangeable calcium were the important factors associated with soil OC and TN accumulation. Soil net N mineralization and nitrification rates were similar to the patterns of soil OC or TN concentrations in grassland to secondary forest. Soil substrate controlled soil N transformation rates along vegetation restoration. Our results suggested that abandoning farmlands for natural vegetation restoration can improve the soil structure, facilitate the coupled accumulation of soil C and N, and enhance soil N transformation rates and N availability, but the coupling accumulation of soil C and N may be limited by soil N in the early stages of vegetation restoration.

1. Introduction

Natural vegetation restoration on abandoned farmlands is widely recognized as an effective approach to improving soil structure and enhancing soil organic carbon (OC) and total nitrogen (TN) stocks. Soil OC sequestration related to vegetation restoration is a possible way to mitigate atmospheric CO_2 and regulate climate change (Singh et al., 2016). Soil OC participates in various physical and biogeochemical processes in soils (Kumar et al., 2018; Wu et al., 2020) and plays a pivotal part in maintaining soil quality and ecosystem functionality (Benbi et al., 2015). For instance, soil OC is a major binding agent in the formation of aggregates (Six et al., 2004; Tisdall and Oades, 1982). The cycling of soil OC is linked to major nutrients, especially N (Wang et al., 2018). Soil N has been considered an important factor in determining long-term soil carbon sequestration following vegetation succession (Song et al., 2019; Wen et al., 2016; Xiao et al., 2018). N is also the major limiting element of net primary production in most terrestrial ecosystems (LeBauer and Treseder, 2008). Thus, understanding soil OC and N status following vegetation succession is important for predicting restoration process, and developing an effective restoration way to mitigate global warming and improve soil quality.

Soil OC and N stock can either increase, decrease, or cause negligible changes after vegetation restoration (Deng et al., 2014a; Li et al., 2012; Liu et al., 2019b). This inconsistent response may be due to the complexity of soil OC and N dynamics, which is affected by different factors such as land use, climate, restoration stages (Deng et al., 2014a; Li et al., 2012), and soil properties (Liu et al., 2019b; Yang et al., 2016) during vegetation restoration. Therefore, considerable uncertainties remain in terms of soil OC and N accumulation, and the mechanisms explaining the soil OC and N dynamics after vegetation restoration are insufficiently understood, especially in karst regions. Soil structure is commonly characterized through aggregate size distribution and stability, which is important not only for carbon turnover, but also for the cycling of nutrients, particularly nitrogen (Schlüter et al., 2020). Soil

** Corresponding author at: Earthquake Agency of Xinxiang City, Xinxiang 453000, People's Republic of China.
E-mail addresses: lanjiacheng@gznu.edu.cn (J. Lan), qningh@126.com (N. Hu).

https://doi.org/10.1016/j.ecoleng.2020.106033
Received 1 February 2020; Received in revised form 23 August 2020; Accepted 26 August 2020
Available online 06 September 2020
0925-8574/

aggregates are closely related to soil OC dynamics and nutrient cycling (Six et al., 2004). Vegetation restoration generally results in soil aggregate formation, increasing macroaggregates, which physically protect soil OC from microbial attack and mineralization (Wei et al., 2012). However, the effects of soil aggregates on soil OC and N accumulation remain unclear in karst regions.

The karst system in Southwest China, famous for its rocky desertification, is one of the most ecologically vulnerable regions due to extensive human activities on extremely fragile geological background (Jiang et al., 2014). The soils in this region have been degraded and eroded, following the conversion of natural vegetation into cropland (Li et al., 2017). The “Grain for Green” program and the Karst Rocky Desertification Restoration Project were conducted to restore the ecosystem in this region (Tong et al., 2018; Yang et al., 2017). Several studies have focused on the effect of vegetation restoration on individual soil physical properties (Yao et al., 2009), soil quality (Zhang et al., 2019b), and soil OC and N accumulation (Hu et al., 2018; Liu et al., 2019b; Xiao et al., 2017a) in this region. After natural vegetation restoration, OC and N accumulate due to the increase in the amount of litter and root biomass in the soils (Deng et al., 2018; Tang et al., 2016; Wei et al., 2012; Zhang et al., 2019a). Nevertheless, most of these studies have concentrated primarily on individual soil OC or N stocks, but knowledge on the coupling of soil OC and N accumulation during vegetation restoration, particularly at an aggregate scale is limited. Several studies have reported that soil N distribution and dynamics in aggregates have trends similar to those in OC (Wang et al., 2018; Zhang et al., 2019a). Soil N is a key factor for determining long-term soil OC accumulation because soil N availability is a major limiting factor after vegetation restoration (Deng et al., 2014b; Liu et al., 2019b). Limited studies have focused on soil N availability and transformations in relation to vegetation succession in karst regions (Li et al., 2017; Liu et al., 2019b; Wen et al., 2016; Xiao et al., 2018; Zhang et al., 2015). The results of these studies are also inconsistent. Soil N cycling indicators may increase, decrease, or not exhibit clear patterns following vegetation succession. For example, soil nitrate (NO_3^-) levels and the rates of net mineralization and nitrification increased in a karst system in Guangxi Zhuang Autonomous Region, Southwest China (Song et al., 2019; Xiao et al., 2018), with the highest increase observed in secondary forest and the lowest increase noted in grassland; however, soil ammonium (NH_4^+) content exhibited no clear patterns during post-agricultural succession. These studies have suggested that soil N availability is not the limiting nutrient for vegetation succession and can sustain soil carbon sequestration for a long period (Song et al., 2019; Wen et al., 2016; Xiao et al., 2018). By contrast, soil carbon is limited by soil N in the initial stage of vegetation restoration in the karst region of Southwest China (Song et al., 2019; Zhang et al., 2015). These inconsistent results are probably due to several factors, such as land use, the plant species present, study scale, and soil properties. Among soil properties, OC, TN, and C:N ratio are generally considered to be the primary factors affecting soil N availability (Booth et al., 2005). In addition, soil exchangeable calcium is the major factor determining soil organic matter (SOM) stability and thus soil C and N levels in a karst region (Li et al., 2017). However, soil N availability dynamics and its influencing factors following vegetation restoration in karst ecosystems are limited and poorly understood.

The karst region in Southwest China spans eight provinces, with various landforms, including mountains, hills, valleys, basins, and plains; the region is characterized by strong heterogeneity and fragmentation (Wang et al., 2019). Therefore, soil C and N dynamics may vary in different karst landforms following vegetation restoration. Previous studies have mainly focused on a karst landscape with gentle valleys flanked with steep hills in the Guangxi Autonomous Region, Southwest China (Li et al., 2017; Liu et al., 2019b; Wen et al., 2016; Xiao et al., 2018; Zhang et al., 2015). Whether similar patterns of soil OC and N dynamics following vegetation restoration in previous studies are found in other karst regions is unclear.

In this study, we select a typical karst trough valley landscape in the Zhongliang Mountains in Chongqing, Southwest China. Soil samples are collected from four natural vegetation restoration successional stages: grassland, shrubland, secondary forest I, and secondary forest II, using farmland as a reference to investigate soil structure parameters, soil N indicators, soil calcium, and soil OC and TN accumulation in whole soil and aggregates. We hypothesize that (1) vegetation restoration improves the soil structure and enhances the OC and TN contents associated with soil aggregates; (2) soil OC and TN are closely coupled and accumulated in whole soil and aggregates, and soil C accumulation may be limited by soil N in the early stages of vegetation restoration; and (3) net soil N mineralization rate (NMR) and N nitrification rate (NNR) are similar to the patterns of soil OC and TN accumulation and controlled by OC, TN, C:N ratio, and exchangeable calcium following natural vegetation restoration.

2. Materials and methods

2.1. Site description

This experiment was conducted in Zhongliang Mountains (24°39′–30°3′ N, 106°18′–106°56′ E) located in the northwest of Chongqing, Southwest China (Figure 1). This area is characterized by a typical subtropical monsoon climate. The mean air temperature is 18 °C. The mean precipitation is 1100 mm, most of which occurs from March to September. In accordance with the Food and Agriculture Organization system, the soil in the study area is calcareous lime soil with a thickness of less than 50 cm in the karst area. This karst region has a total land area of 38.5 km^2 (mainly forestland and agricultural land) and ranges in elevation from 500 m to 700 m above sea level (Liu et al., 2019a). Vegetation is mostly subtropical evergreen wide-leaf forests and shrubs. The “Grain for Green” project launched in the middle of the 1990s in this area has resulted in most farmland abandonment and forest restoration. Thus, karst rocky desertification has been effectively controlled, and the desert covers an area of approximately 0.39 km^2 in this region.

2.2. Field sampling

This study consisted of four natural vegetation restoration successional stages, namely, grassland, shrubland, secondary forest I, and secondary forest II, with farmland as the control. According to the local elderly people, the four natural vegetation restoration successional stages in the area were farmlands abandoned approximately 8, 20, 35, and > 50 years ago that had turned into grassland, shrubland, secondary forest I, and secondary forest II, respectively. The farmlands had been planted with maize for at least 100 years. All these successional stages were distributed with the elevation from 650 m to 670 m. The detailed description of the four successional stages was as follows:

a) Grassland: The main plant species was *Imperata cylindrica* (L.) Beauv., accompanied by *Lonicera japonica* Thunb. The mean height of grass was 0.9 m. The vegetation coverage was 75%.
b) Shrubland: The dominant species were *Quercus acutissima* Carruth. and *Alchornea davidii* Franch. Lianas grew vigorously in this site. The height of trees ranged from 3 to 5 m. The diameter breast height of trees ranged from 6 cm to 15 cm. The vegetation coverage was 60%.
c) Secondary forest I: It comprised shrub and arbor species, deciduous forest, and broadleaf evergreen forest, including mostly *Robinia pseudoacacia* L., *Broussonetia papyrifera* (L.) Vent. and *Trachycarpus fortunei* (Hook.) H. Wendl. The height of trees ranged from 7 m to 12 m. The diameter breast height of trees ranged from 12 cm to 20 cm. The vegetation coverage was 70%.
d) Secondary forest II: The vegetation was mainly dominated by *Cyclobalanopsis glauca* (Thunb.) Oerst., *Cinnamomum camphora* (L.) Presl., and *Cupressus funebris* Endl, including evergreen broadleaf

and evergreen coniferous forests. The height (13–16 m) and diameter breast height (20–35 cm) of trees in this successional stage were higher than those in secondary forest I. The vegetation coverage was 80%.

For each vegetation type, two farmland plots (5 m × 5 m), two grassland plots (10 m × 10 m), two shrubland plots (10 m × 10 m), three secondary forest I plots (10 m × 10 m), and two secondary forest II plots (20 m × 20 m) were established in November 2013. Three undisturbed soil samples were randomly collected at a depth of 0–10 cm in each plot and mixed into one sample, taken to the laboratory, and air dried to determine soil physicochemical properties. Soils were also sampled using stainless steel cylinders (100 cm^3) to determine the bulk density (BD) in each plot.

2.3. Laboratory analysis

The fresh and undisturbed soils were broken into < 10 mm particles by hand along natural failure surfaces. After air drying, the soils were separated by dry sieving through 10, 5, 2, 1, and 0.25 mm sieves to obtain each aggregate size class in accordance with the method described by ISSAS (1978). The air-dried soil samples were sieved through 0.25 mm sieves to measure the OC and TN concentrations. The light and heavy fractions were separated using the density fractionation method as described by (Lu, 2000). The OC and light-fraction OC concentrations were measured through oxidation with KCr_2O_7 + H_2SO_4 and titration with $FeSO_4$ (Lu, 2000). The TN and mineral N concentrations were determined in accordance with a method described by Lu (2000). The TN concentration was measured via the Kjeldahl method. Ammonium nitrogen (NH_4^+–N) and nitrate nitrogen (NO_3^-–N) were determined using the indigo blue colorimetric method and ultraviolet spectrophotometry, respectively. Air-dried samples were sieved to 2 mm to measure soil clay content via a simple hydrometer method. BD was measured using the gravimetric method. Exchangeable Ca contents were measured through a modified procedure developed by Lu (2000). Briefly, 2.0 g of soils were placed in 100 mL centrifuge tubes, and extracted using 1 mol L^{-1} ammonium acetate at pH 7.0. The supernatant was centrifuged (5 min, 4000 rpm) several times until no calcium reaction occurred. The collected supernatant was analyzed by ICP-OES (Inductively Coupled Plasma Optical Emission Spectr, Thermo Fisher Scientific, USA) to measure exchangeable Ca.

The NMR, net ammonification rate (NAR), and NNR were determined using a modified resin core incubation technique under field conditions as described by Bhogal et al. (1999). The resin core consisted of a soil core (PVC cylinder, 45 mm diameter × 150 mm length) with the bottom 2 cm of the soil removed and replaced with a nylon mesh bag containing 4 g of an anion-exchange resin that was sandwiched between two filter papers. A gypsum block with a drainage hole was placed below the resin bag to prevent the exchange of nitrate from the subsoil onto the resin and ensure smooth drainage. Four cores (one core with nothing, and three replicate resin cores) were set at each sampling plot and buried in the soil at a depth of 12 cm at the beginning of each incubation time. Each core was 20 cm apart. The three replicate resin cores were retained in the soil for 4 weeks in the field, and the other core was taken to the laboratory for analysis of the initial soil mineral nitrogen contents (NO_3^-–N and NH_4^+–N). The NMR and NNR were measured in January, April, July, and October 2013. Therefore, a total of 16 cores were established in each plot. At the end of the incubation period, the resin cores were removed from the soil and taken back to the laboratory for determination of NO_3^-–N and NH_4^+–N in core soils and the adsorbed NO_3^-–N by anion resin. NO_3^-–N held by the resin was extracted by shaking each bag with 50 mL of 2 mol L^{-1} KCl solution in 1 h. The extracts were filtered using glass fiber filters. The NMR, NAR, and NNR were determined as the difference in NO_3^-–N and NH_4^+–N contents at the beginning and end of the incubation and NO_3^-–N in the anion-exchange resin. We used the average value of four (four incubation periods) determinations for analysis in this study.

Soil OC and TN stocks (kg m^{-2}) were calculated as follows:

$$\text{Soil OC stocks} = \frac{\text{OC} \times \text{D} \times \text{BD}}{100},$$

$$\text{Soil TN stocks} = \frac{\text{TN} \times \text{D} \times \text{BD}}{100},$$

where soil *OC* is the OC concentration (g kg^{-1}), soil *TN* is the TN concentration (g kg^{-1}), *D* is the thickness (cm) of soil depth, and *BD* is the bulk density (g cm^{-3}).

OC and TN stocks (kg m^{-2}) in each aggregate size class were calculated as follows:

$$\text{Stocks of OC}_i = \frac{\text{OC}_i \times \text{w}_i \times \text{D} \times \text{BD}}{10},$$

$$\text{Stocks of TN}_i = \frac{\text{TN}_i \times \text{w}_i \times \text{D} \times \text{BD}}{10},$$

where OC_i is the OC concentration in the *ith* aggregate size fraction (g kg^{-1} aggregate), TN_i is the TN concentration in the *ith* aggregate size fraction (g kg^{-1} aggregate), and w_i is the total soil proportion in the *ith* aggregate size fraction (%).

2.4. Statistical analyses

One-way ANOVA, followed by least-significant difference, was used to examine and compare the differences in soil indicators among diverse vegetation types at the $P < 0.05$ level. The relationships among soil variables were tested through Pearson correlation analyses. All statistical analyses were performed using SPSS 17.0 and OriginPro (version 8.0) for Windows.

3. Results

3.1. Soil structures

The aggregates were dominated by 5–10 mm and 2–5 mm fractions for all vegetation types. Compared with farmland, the proportion of 5–10 mm fraction significantly increased from grassland to shrubland, secondary forest I and secondary forest II. However, the proportion of 2–5 mm fraction in farmland was significantly higher than that in shrubland and secondary forest in addition to grassland. No significant difference was noted in the proportions of 1–2 mm, 0.25–1 mm and < 0.25 mm fractions among vegetation types. MWD and MGD values were the lowest in the farmland, but no difference was observed among the four vegetation successional stages.

3.2. OC and N indicators in whole soil

Compared with farmland, natural vegetation restoration patterns exhibited significantly greater OC and TN concentrations in the 0–10 cm soil depth (Tables 2 and 3). Generally, the OC concentrations and stocks gradually increased from farmland (16.77 ± 1.75 g kg^{-1}, 1.96 ± 0.25 kg m^{-2}) to secondary forest II (32.16 ± 2.37 g kg^{-1}, 3.68 ± 0.20 kg m^{-2}) along the vegetation successional stages. The TN concentrations and stocks exhibited similar patterns to OC concentrations and stocks, with the highest concentrations recorded in secondary forest II (2.61 ± 0.28 g kg^{-1}, 299.04 ± 26.92 g m^{-2}) and the lowest concentrations observed in farmland (1.52 ± 0.13 g kg^{-1}, 178.14 ± 20 g m^{-2}). No significant difference was observed in soil OC and TN concentrations and stocks between farmland and grassland. Moreover, soil TN concentration in shrubland did not markedly change relative to those in grassland and farmland.(Table 3)

Soil mineral N significantly varied following vegetation restoration (Fig. 2, $P < 0.05$). Soil NO_3^-–N concentration decreased initially from farmland to grassland but increased from grassland to shrubland and

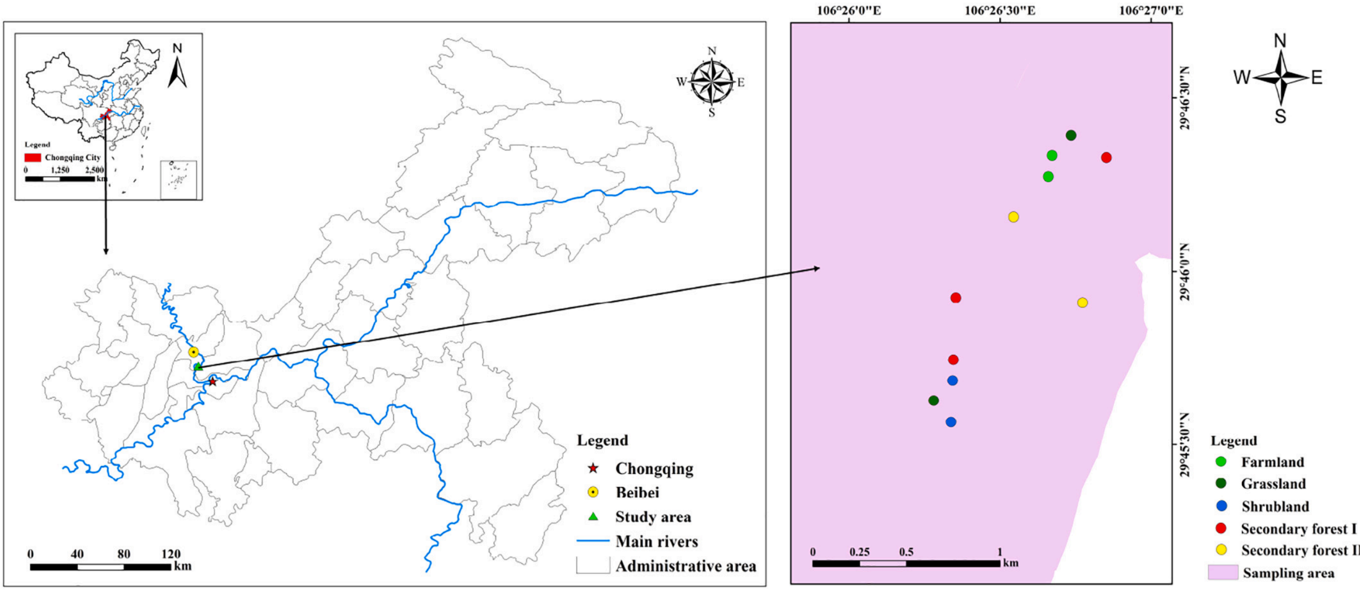

Fig. 1. Location of study area and distribution of sampling sites.

secondary forest. Soil NO_3^-–N concentration was significantly higher in secondary forest I (5.75 ± 1.06 mg kg^{-1}) compared with those in the other successional stages. Soil NH_4^+–N concentrations were significantly higher in secondary forest II, secondary forest I, and shrubland compared with that in farmland. No significant difference was observed in soil NH_4^+–N concentrations between farmland and grassland. The soil NO_3^-–N:NH_4^+–N ratio significantly decreased initially from farmland to grassland and then increased from grassland to secondary forest I, after which it significantly decreased. The soil NO_3^-–N:NH_4^+–N ratios in farmland and secondary forest I were > 1, but no significant difference was observed between them.

The NMR, NAR, and NNR were significantly different following vegetation restoration (Fig. 2). The NMR decreased from farmland to grassland, but it increased significantly from grassland to shrubland, secondary forest I, and secondary forest II. The NNR initially significantly decreased from farmland to grassland and then significantly increased to shrubland, and secondary forest I but greatly decreased in secondary forest II. The NAR was highest in secondary forest II and significantly higher than those in the other successional stages, but no significant difference was observed among other vegetation successional stages.

3.3. OC and TN in soil aggregates

The OC concentration showed a significant difference in each aggregate fraction among vegetation types (Table 2), with the highest concentration observed in secondary forest II and the lowest concentration recorded in farmland. The increases in OC concentrations of 5–10 mm and < 0.25 mm aggregates were greater than those of 2–5 mm, 1–2 mm, and 0.25–1 mm aggregates following vegetation restoration. The patterns of these changes were similar to those of OC concentrations in whole soil (Table 2). Aggregate-associated TN concentrations also followed these patterns of OC concentrations (Table 3). The concentrations of aggregate-associated OC and TN presented a clear trend, in which large aggregates have lower OC and TN concentrations compared with small aggregates following vegetation restoration; the order was as follows: 5–10 mm < 2–5 mm < 1–2 mm < 0.25–1 mm < 0.25 mm (Tables 2, 3).

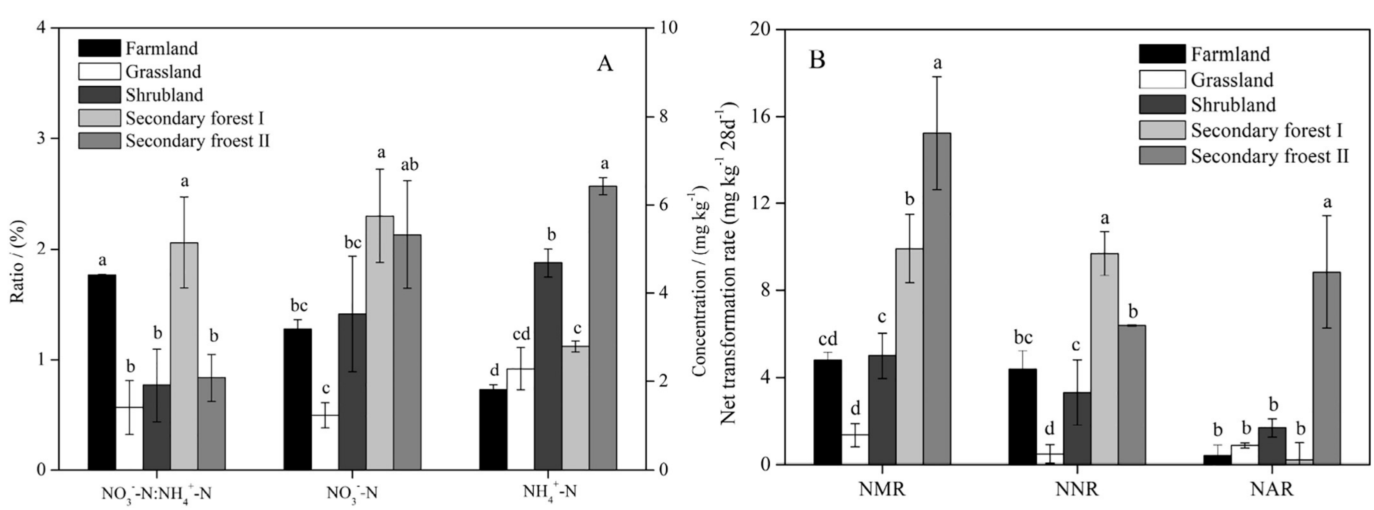

Fig. 2. Variations in (A) soil NO_3^-–N:NH_4^+–N ratio (F = 11.51, P = 0.006), NO_3^-–N (F = 8.11, P = 0.013) and NH_4^+–N (F = 14.5, P = 0.003) concentrations, and (B) in soil net N mineralization rate (NMR: F = 27.19, P < 0.01), net N nitration rate (NNR: F = 34.05, P < 0.001) and net N ammonification rate (NAR: F = 20.01, P < 0.01) following vegetation restoration succession. The error bars are mean standard errors (farmland, grassland, shrubland, secondary forest II, n = 2; secondary forest I, n = 3). The different lowercase letters indicate significant differences among vegetation types (P < 0.05).

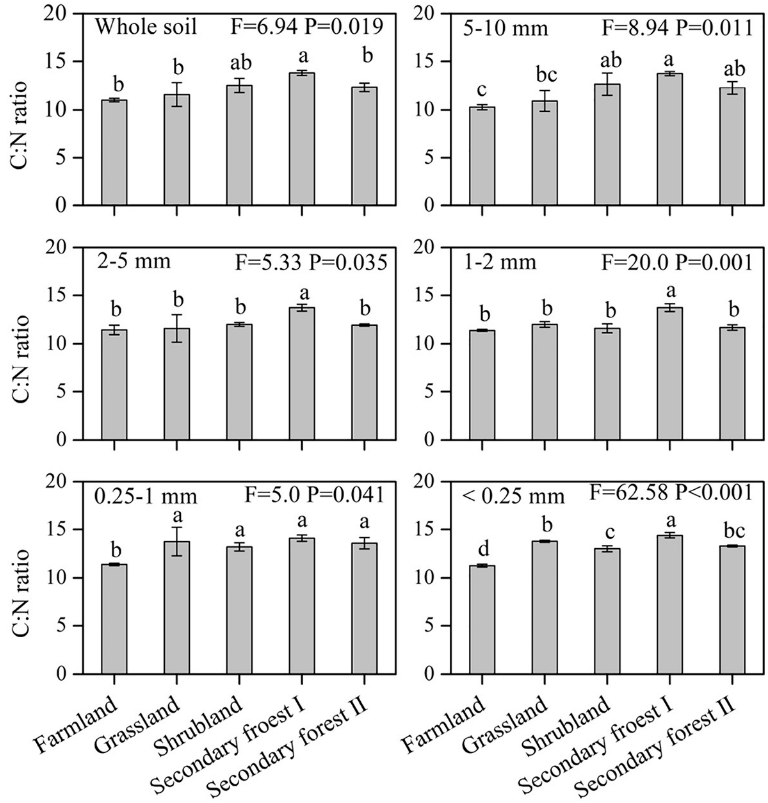

Fig. 3. C:N ratios in whole soil and aggregates along vegetation restoration succession. The error bars are mean standard errors. The different lowercase letters indicate significant differences among vegetation types ($P < 0.05$).

The changes in aggregate-associated OC and TN stocks in the 5–10 mm and 2–5 mm aggregates were significantly affected by vegetation types, but they had no significant changes and no clear patterns in the 1–2 mm, 0.25–1 mm, and < 0.25 mm aggregate fractions (Tables 2, 3). Compared with the OC and TN stocks in farmland, those in the 5–10 mm aggregate fraction significantly increased from grassland to secondary forest along the vegetation successional stages. In the 2–5 mm aggregate fraction, the OC and TN stocks were significantly higher in secondary forest II compared with those in farmland, but no significant difference was observed between farmland and other vegetation successional stages.

3.4. C:N ratios in whole soil and aggregates

The soil C:N ratios in whole soil and each aggregate fraction were significantly different among vegetation types, with the highest ratios recorded in secondary forest I and the lowest ratios observed in farmland (Fig. 3). The soil C:N ratio in whole soil significantly increased in secondary forest I relative to that in farmland (Fig. 3). The soil C:N ratio significantly increased in the 5–10 mm aggregate fraction from shrubland to secondary forest II and in the 0.25–1 mm and < 0.25 mm aggregate fractions from grassland to secondary forest II. In the 2–5 mm and 1–2 mm, the C:N ratios were significantly higher in secondary forest I compared with those in farmland. The soil C:N ratios seemed to follow an increasing trend from large aggregates to small aggregates, with high values recorded in the 0.25–1 mm and < 0.25 mm aggregates (Fig. 3).

3.5. Relationships between soil structure parameters and properties

Correlation analysis demonstrated that clay and exchangeable calcium contents were related positively to MWD, MGD, and the proportion of 5–10 mm aggregates but negatively to the proportions of 2–5 mm and 1–2 mm aggregates (Table 4). Meanwhile, no statistical relationships were found between them and the proportions of 0.25–1 mm and < 0.25 mm aggregates (Table 4). No significant correlation existed between OC concentration and MWD, MGD and the proportion of > 0.25 mm aggregates (Table 4). MWD and MGD were related positively to the proportion of 5–10 mm aggregates but negatively to the proportions of 2–5 mm, 1–2 mm and 0.25–1 mm aggregates (Table 4).

3.6. Relationships between OC and TN, and factors affecting OC and TN accumulation

Highly positive relationships existed between OC and TN concentrations in whole soil and different aggregate fractions (Fig. 4). Highly positive relationships were also observed between OC and TN stocks in whole soil and different aggregate fractions.

The soil OC and TN stocks correlated positively with the OC and TN stocks in large aggregates (5–10 mm and 2–5 mm, Fig. 5, $P < 0.01$) but insignificantly (1–2 mm and 0.25–1 mm) or only slightly (< 0.25 mm, $P < 0.05$) with the OC and TN stocks in small aggregates (Fig. 5). Therefore, the accumulation of OC and TN in total soil tended to be dependent on OC and TN stocks in large aggregates. The soil C:N ratio was significantly positively correlated with the concentrations and stocks of soil OC and TN (Table 5). Soil exchangeable calcium content was found to have a close relationship with OC and TN concentrations and stocks. Soil pH was correlated positively with soil OC concentrations and stocks but insignificantly with soil TN concentrations and stocks.

3.7. Factors affecting soil N transformation

The results from correlation analysis showed that soil N variables were significantly correlated with soil OC, TN, and C:N ratio (Table 5).

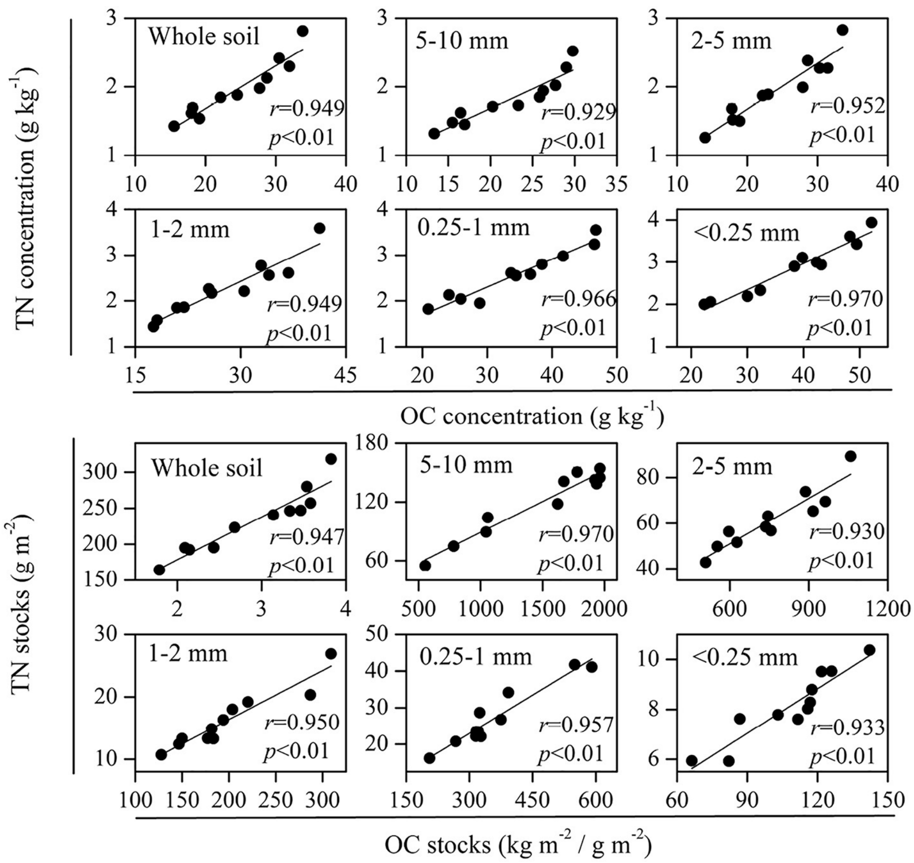

Fig. 4. Correlations between soil OC and TN in aggregates and whole soil along vegetation restoration succession OC: organic carbon; TN: total nitrogen.

The NO_3^-–N and NNR were significantly correlated with OC, TN, C:N ratio, exchangeable calcium content and pH. NMR, NH_4^+–N and NAR were positively related to soil OC and TN, whereas they exhibited no significant correlations with C:N ratio, exchangeable calcium content and pH. NH_4^+–N showed a significant positive correlation with NMR and NNR, but no correlation with NNR. A significant correlation was found among NMR and NNR, and NAR.

4. Discussion

4.1. Improvement in soil structure

Several studies have shown that vegetation restoration or afforestation after farmland abandonment or the conversion of farmland into forest significantly increases the amounts of macroaggregates but decreases the quantity of microaggregates (Deng et al., 2018; Wei et al., 2012; Zhong et al., 2019). For example, the conversion from farmland to 42-year three afforestation soils in Loess Plateau, China significantly increased in the proportions of macroaggregates (> 2 mm) and mesoaggregates (2–0.25 mm) and the values of MWD and GMD (Zhong et al., 2019). In the same region, Deng et al. (2018) found that macroaggregate (0.25–2 mm) amounts increased from 56.2% to 73.9% and microaggregate (≤0.25 mm) amounts decreased from 43.8% to 26.2% in topsoil (0–10 cm). Similar results were observed in our study, but some differences existed in the changes in aggregate fractions. In the present study, natural vegetation restoration significantly increased in the proportion of 5–10 mm aggregates and the values of MWD and MGD relative to farmland. This increase indicated that vegetation restoration on abandoned farmlands enhanced large aggregates and the stability of soil aggregates. In addition, we observed significant correlations among MWD, MGD, and the proportion of 5–10 mm aggregates (Table 4), suggesting that the effect of natural vegetation restoration on soil aggregate stability was mainly determined by the changes in the amounts of 5–10 mm aggregates. This result supported our first hypothesis that natural vegetation restoration on abandoned farmlands improves soil structure. This improvement may be due to reduced destruction and increased input of plant residues (e.g., litter or root biomass and exudates), which promote the aggregation of soil particles (Tisdall and Oades, 1982; Wei et al., 2012). SOM is a major binding agent for the formation and stabilization of aggregates (Six et al., 2002; Six and Paustian, 2014). Several studies have reported that soil OC concentration has a strong relationship with aggregate amounts and stabilization (Deng et al., 2018; Six et al., 2002; Tang et al., 2016; Zhong et al., 2019; Zhu et al., 2017). Nevertheless, we did not find significant relationships between OC concentration and aggregate amount, MWD, and MGD. This result indicated that other agents, such as clay or exchangeable calcium content, influence the aggregation of soil particles. Ge et al. (2019) found that the proportions of macroaggregates and microaggregates linearly increase and decrease with clay content, respectively. We also observed that clay content had a significant positive correlation with the 5–10 mm aggregate amount, MWD and MGD ($P < 0.01$), but we observed a negative correlation with the proportions of other aggregate sizes (Table 4). Moreover, a similar pattern was observed between exchangeable calcium content and each aggregate amount (Table 4). Large aggregates (> 1 mm) were significantly influenced by vegetation types ($P < 0.05$), whereas small aggregates (0.25–1 mm and < 0.25 mm) were more stable than the large aggregates (Table 1). This finding is consistent with the results of Xiao et al. (2017b) in a karst region in Guangxi Autonomous Region, Southwest China.

4.2. Soil OC and TN accumulation

This study showed that total soil OC concentration increased by an

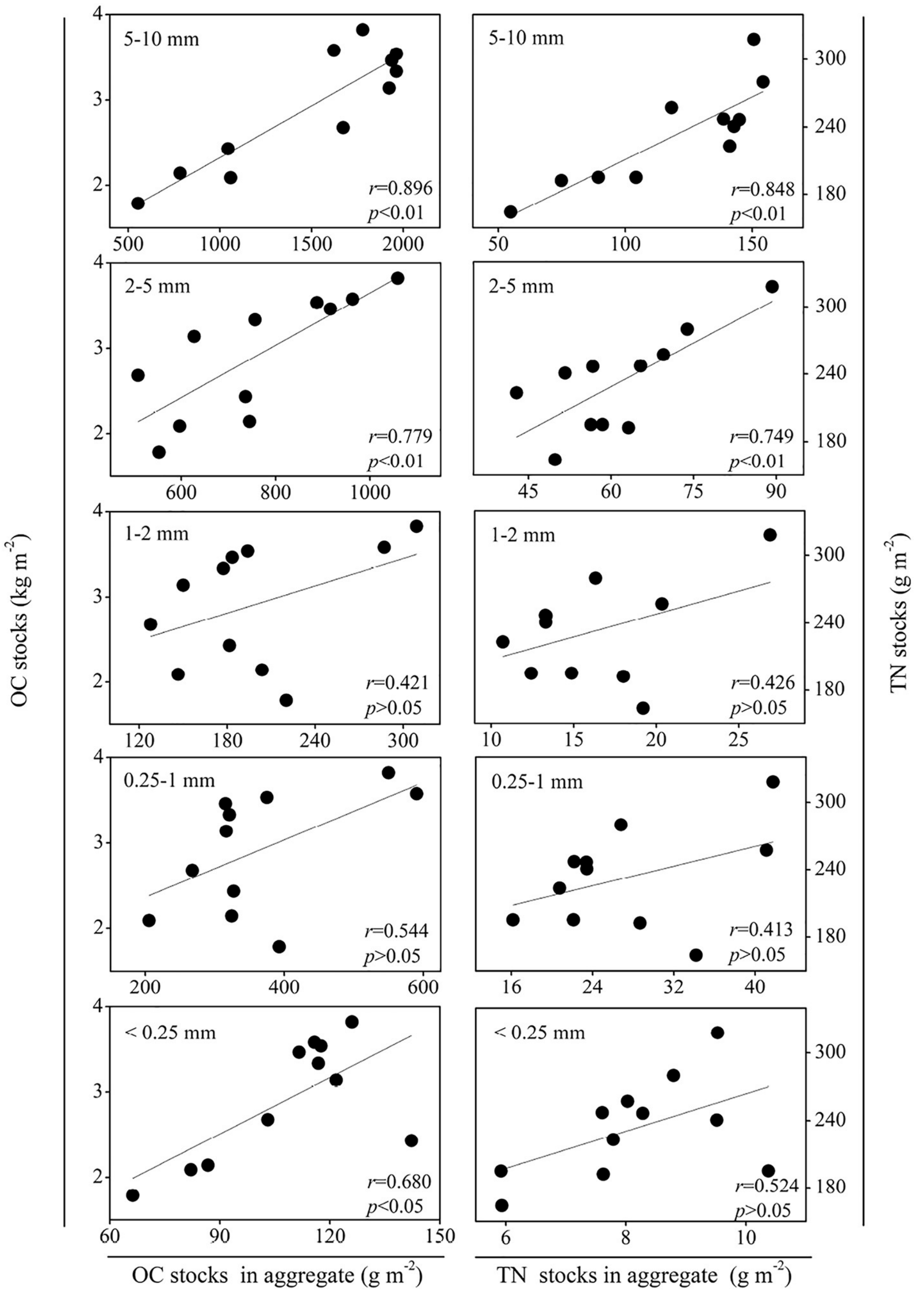

Fig. 5. Correlations between OC stocks in total soil and aggregates and between TN stocks in total soil and aggregates along vegetation restoration succession. OC, organic carbon; TN, total nitrogen.

Table 1
Parameters for soil structure under different vegetation types.

Parameters	Vegetation types					One-way ANOVA results	
	Farmland	Grassland	Shrubland	Secondary forest I	Secondary forest II		
5–10 mm (%)	39.31 ± 4.48c	52.24 ± 5.22b	66.35 ± 2.64a	58.87 ± 6.15ab	55.61 ± 3.84ab	F = 8.41	P = 0.012
2–5 mm (%)	34.65 ± 0.38a	29.92 ± 1.07ab	20.14 ± 1.71d	25.05 ± 3.10c	27.34 ± 0.83bc	F = 14.89	P = 0.003
1–2 mm (%)	9.38 ± 1.69	6.97 ± 1.64	4.34 ± 0.37	5.42 ± 1.34	5.86 ± 1.10	F = 4.32	P = 0.055
0.25–1 mm (%)	13.82 ± 3.55	7.91 ± 1.44	6.88 ± 0.43	8.47 ± 2.48	9.08 ± 1.88	F = 2.85	P = 0.121
< 0.25 mm (%)	2.85 ± 0.37	2.97 ± 1.07	2.31 ± 0.12	2.18 ± 0.17	2.12 ± 0.03	F = 1.46	P = 0.324
MWD (mm)	4.39 ± 0.30b	5.12 ± 0.32a	5.79 ± 0.13a	5.43 ± 0.34a	5.27 ± 0.23a	F = 6.58	P = 0.022
MGD (mm)	3.13 ± 0.30b	3.90 ± 0.44a	4.60 ± 0.16a	4.22 ± 0.39a	4.06 ± 0.29a	F = 5.05	P = 0.040

MWD, mean weight diameter; MGD, geometric mean diameter; Different lowercase letters in the same row indicate significant difference among different vegetation types ($P < 0.05$).

average of 54%, and OC stock increased by an average of 57%, following a natural vegetation restoration of an abandoned farmland. In the farmland, the low OC concentration and stock obtained were expected because of the low input and high decomposition rate of organic matter (Qiu et al., 2015). By contrast, natural vegetation restoration enhanced the accumulation of litter and root biomass in the soils (Deng et al., 2018; Tang et al., 2016; Wei et al., 2012; Zhang et al., 2019a). In the present study, the total soil OC concentrations and stocks significantly increased from grassland and shrubland to secondary forest. This result indicated that soil OC accumulation may be determined by the plant species present in the area. Our previous study in the same region showed that litter decomposition coefficient and OC release rate increased in the order of grassland (0.73, 58.5%) < shrubland (0.9, 61.7%) < secondary forest (1.27, 72.1%), following vegetation succession (Hu et al., 2016). Moreover, a positive correlation was found between litter decomposition coefficient and soil OC concentration following vegetation succession (Hu et al., 2016). Thus, the high litter decomposition and OC release rates increased the OC input to the soils, thereby promoting soil OC accumulation. In addition, the C:N ratios in whole soil tended to increase from farmland, grassland, and shrubland to secondary forest (Fig. 3). A high C:N ratio may inhibit microbial decomposition (Deng et al., 2014b), thereby stimulating soil C and N accumulation. By contrast, the low C:N ratio in the farmland indicated that the soil had a high potential to decompose (Qiu et al., 2015). However, the soil OC and TN levels between farmland and grassland were insignificant. Similar results were reported by Hu et al. (2018) in another karst region. Moreover, the soil TN concentration in shrubland did not significantly change relative to those in grassland and farmland. This result was expected due to the low productivity of new vegetation in early years (Laganière et al., 2010). Therefore, the time since the farmland was abandoned and plant species play a key role in determining soil OC and N accumulation.

Similar patterns with OC concentrations and stocks were observed for soil N concentrations and stocks following vegetation succession in the present study because most soil N is a composition of SOM. Additionally, the total soil OC and TN concentrations were highly correlated (Fig. 4) in the present study, indicating that the coupling of soil OC and TN accumulation may exist. Several studies have found that soil C and N are closely accumulated (Hu et al., 2018; Li et al., 2012; Liu et al., 2019b). In the present study, similar and strong correlations between OC and TN were also observed in each soil aggregate (Fig. 4, $P < 0.01$). This finding confirmed that OC accumulation is closely coupled with TN accumulation. The change in soil C:N ratio was highly constrained by the soil C and N and the accumulation and decomposition of organic matter (Knops and Tilman, 2000; Miller et al., 2004). Total soil OC and TN significantly increased after farmland abandonment (Tables 2, 3), and the increase was greater in OC compared with that in TN. For example, the OC stocks increased by 15% in grassland, 48% in shrubland, 76% in secondary forest I, and 87% in secondary forest II. By contrast, the TN stocks increased by 10% in grassland, 30% in shrubland, 41% in secondary forest I, and 68% in secondary forest II. SOM accumulation results in an increase in soil C:N ratio (Post et al., 1985), and a low TN accumulation leads to a high C:N ratio (Liu et al., 2019b). We also found that the C:N ratios in whole soil and aggregates were higher in natural vegetation restoration compared with those in the farmland (Fig. 3), and the average increase was significantly higher than 1 ($P < 0.05$, one-sample *t*-test). The increase in soil C:N ratio following vegetation restoration implies that the increase in soil OC sequestration may be faster than N sequestration but may be limited by soil N (Liu et al., 2019b). N limitation reportedly constrained soil OC accumulation during the early stages of vegetation restoration in other karst regions in Southwest China (Liu et al., 2019b; Zhang et al., 2015). The NO_3^-–N:NH_4^+–N ratio can be used to determine the abundance or limitation of soil N availability (Wen et al., 2016; Xiao et al., 2018). In the present study, the NO_3^-–N:NH_4^+–N ratios gradually increased from grassland to shrubland to secondary forest I, but the ratios were less than 1 in grassland and shrubland. These results indicated that soil N limitation exists in the early stages of vegetation restoration. Therefore, soil N input should be increased in the early stages of natural vegetation restoration in degraded karst ecosystems. The results of soil OC and TN accumulation support our second hypothesis (2).

4.3. Factors affecting soil OC and TN accumulation

Given that most soil N is in the form of SOM, the mechanisms that enhance SOM stabilization, in turn, increase soil N retention (Wen et al., 2016). SOM is affected by several factors, such as land use, climate, plant species, restoration time (Laganière et al., 2010; Li et al., 2012), and soil variables (Yang et al., 2016), during vegetation restoration. The effects of soil variables, particularly OC and TN associated with soil aggregates, and calcium on total soil OC and TN accumulation are poorly understood in karst regions. In the present study, the soil OC and TN stocks correlated positively with the OC and TN stocks in large aggregates (5–10 mm and 2–5 mm, Fig. 5, $P < 0.01$) but insignificantly (1–2 mm and 0.25–1 mm) or only slightly

Table 2
OC concentrations and stocks in whole soil and aggregates along vegetation restoration succession.

Vegetable types	Whole soil	Aggregate sizes				
		5–10 mm	2–5 mm	1–2 mm	0.25–1 mm	< 0.25 mm
OC concentrations ($g\cdot kg^{-1}$)						
Farmland	16.77 ± 1.75c	14.41 ± 1.53e	15.95 ± 2.79c	19.53 ± 1.99b	22.51 ± 2.26c	22.90 ± 0.78c
Grassland	18.66 ± 0.69c	16.70 ± 0.34d	18.35 ± 0.78bc	19.77 ± 3.08b	27.39 ± 2.06bc	31.17 ± 1.61c
Shrubland	23.33 ± 1.68b	21.78 ± 2.15c	22.57 ± 0.54b	25.69 ± 0.29b	34.06 ± 0.54ab	39.08 ± 1.00b
Secondary forest I	29.47 ± 2.22a	26.61 ± 0.99b	29.87 ± 1.81a	33.79 ± 3.16a	40.55 ± 5.26a	44.98 ± 3.91ab
Secondary forest II	32.16 ± 2.37a	29.39 ± 0.54a	32.50 ± 3.51a	39.04 ± 5.89a	46.64 ± 3.57a	50.79 ± 2.72a
One-way ANOVA results	F = 26.32	F = 55.49	F = 21.86	F = 12.21	F = 13.29	F = 35.29
	$P = 0.001$	$P < 0.001$	$P = 0.001$	$P = 0.005$	$P = 0.004$	$P < 0.001$
OC stocks ($kg\cdot m^{-2}$ for whole soil, $g\cdot m^{-2}$ for aggregates)						
Farmland	1.96 ± 0.25c	668.52 ± 161.95c	648.7 ± 135.7bc	212 ± 11.68	358.5 ± 48.31	76.53 ± 14.50
Grassland	2.26 ± 0.24c	1051.6 ± 10.04b	666.4 ± 98.71bc	164.1 ± 24.77	266.3 ± 86.08	112.2 ± 42.52
Shrubland	2.91 ± 0.33b	1797.6 ± 177.42a	567.7 ± 84.08c	138.9 ± 15.71	292.1 ± 34.54	112.4 ± 13.19
Secondary forest I	3.46 ± 0.12a	1840.6 ± 189.6a	878.6 ± 108.3ab	215.9 ± 61.64	408.9 ± 157.2	114.8 ± 2.78
Secondary forest II	3.68 ± 0.20a	1870.9 ± 129.6a	973.1 ± 121.2a	251.5 ± 81.35	462.4 ± 123.8	121.8 ± 5.98
One-way ANOVA results	F = 23.69	F = 26.43	F = 5.10	F = 1.61	F = 1.09	F = 1.72
	$P = 0.001$	$P = 0.001$	$P = 0.039$	$P = 0.286$	$P = 0.440$	$P = 0.263$

Different lowercase letters in the same column indicate significant differences among vegetation types ($P < 0.05$), no lowercase letter in the same column represented no significant differences among vegetation types ($P > 0.05$).

Table 3
TN concentrations and stocks in whole soil and aggregates along vegetation restoration succession.

Vegetable types	Whole soil	Aggregate sizes				
		5–10 mm	2–5 mm	1–2 mm	0.25–1 mm	< 0.25 mm
TN concentrations ($g \cdot kg^{-1}$)						
Farmland	1.52 ± 0.13c	1.40 ± 0.11d	1.39 ± 0.18d	1.72 ± 0.19c	1.98 ± 0.22c	2.03 ± 0.04c
Grassland	1.62 ± 0.11c	1.54 ± 0.12 cd	1.59 ± 0.13 cd	1.65 ± 0.30c	2.00 ± 0.06c	2.26 ± 0.10c
Shrubland	1.86 ± 0.03bc	1.72 ± 0.01bc	1.88 ± 0.01bc	2.22 ± 0.06bc	2.58 ± 0.04bc	3.01 ± 0.15b
Secondary forest I	2.13 ± 0.16b	1.94 ± 0.09b	2.18 ± 0.16b	2.46 ± 0.22b	2.87 ± 0.34ab	3.12 ± 0.27b
Secondary forest II	2.61 ± 0.28a	2.40 ± 0.17a	2.55 ± 0.32a	3.10 ± 0.58a	3.40 ± 0.40	3.69 ± 0.23a
One-way ANOVA results	F = 14.43	F = 26.47	F = 14.05	F = 8.45	F = 8.86	F = 26.12
	P = 0.003	P = 0.001	P = 0.003	P = 0.012	P = 0.011	P = 0.001
TN stocks ($g \cdot m^{-2}$)						
Farmland	178.14 ± 20c	64.84 ± 14.11c	56.49 ± 9.44b	18.61 ± 0.85	31.42 ± 3.90	6.78 ± 1.19
Grassland	195.11 ± 0.09c	96.80 ± 10.46b	57.38 ± 1.48b	13.65 ± 1.73	19.14 ± 4.21	8.15 ± 3.15
Shrubland	231.94 ± 12.37b	142 ± 1.17a	47.24 ± 6.23b	12.01 ± 1.83	22.09 ± 1.90	8.65 ± 1.22
Secondary forest I	250.34 ± 6.02b	133.9 ± 13.97a	63.87 ± 6.55b	15.66 ± 4.06	28.90 ± 10.60	7.97 ± 0.34
Secondary forest II	299.04 ± 26.92a	152.43 ± 2.57a	81.57 ± 10.91a	21.61 ± 7.48	34.27 ± 10.59	9.16 ± 0.52
One-way ANOVA results	F = 20.57	F = 26.12	F = 5.88	F = 1.86	F = 1.31	F = 0.72
	P = 0.001	P = 0.001	P = 0.028	P = 0.237	P = 0.364	P = 0.607

Different lowercase letters in the same column indicate significant differences among vegetation types ($P < 0.05$), no lowercase letter in the same column represented no significant differences among vegetation types ($P > 0.05$).

(< 0.25 mm, $P < 0.05$) with the OC and TN stocks in small aggregates (Fig. 5). Additionally, high OC and TN stocks were observed in large aggregates (5–10 mm and 2–5 mm, Tables 2, 3). These results indicated that the total soil OC and TN accumulation was mainly due to the increases in OC and TN in large aggregates following natural vegetation restoration. Vegetation restoration enhances the amount and stability of large soil aggregates, thereby accelerating the incorporation of OC and TN associated with smalle aggregate fractions into large fractions and thus physically protecting them.

Soil properties determine soil OC and N accumulation by influencing the stability and decomposition of SOM (von Lützow et al., 2006). In the present study, the soil C:N ratio was significantly positively correlated with soil OC and TN accumulation. SOM with a low C:N ratio usually decomposes faster than that with a high C:N ratio (Li et al., 2017). The increase in soil C:N ratio following vegetation restoration implies that vegetation restoration slows down SOM decomposition, thereby enhancing soil OC and N sequestration. SOM (including OC and N) was found to have a close relationship with soil exchangeable calcium content in karst regions (Li et al., 2017; Wen et al., 2016; Xiao et al., 2017a; Yang et al., 2016). The same result was obtained in the current study (Table 5). Therefore, the high levels of calcium were likely responsible for the high soil OC and TN concentrations and stocks in shrubland and secondary forest. Soil calcium can act as a polyvalent cation bridge between SOM and mineral surfaces and thus enhance SOM stabilization (Kaiser et al., 2011). In addition, a significant correlation between soil exchangeable calcium and the amount of 5–10 mm aggregates, MWD, and MGD was observed (Table 4), suggesting that soil exchangeable calcium can promote the formation and stabilization of large aggregates (5–10 mm). Soil pH was positively correlated with soil OC concentration and stock (Table 5) probably due to its high correlation with soil exchangeable calcium content.

4.4. Patterns of soil N transformation and its controlling factors

This study showed that NMR and NNR were similar to the patterns of soil OC or TN concentrations from grassland to secondary forest, hence supporting our third hypothesis. Similar patterns were observed in other karst regions in Guangxi Autonomous Region, Southwest China (Xiao et al., 2018). We found that soil inorganic N ($NO_3^- + NH_4^+$) concentration increased with vegetation succession (Fig. 2A). These findings indicated that NMR significantly increased following vegetation restoration, suggesting that natural vegetation restoration can promote soil N transformations and availability. Net soil N transformations are primarily affected by the quality and quantity of the substrate, including soil OC, TN, NH_4^+ availability, and C:N ratio (Booth et al., 2005). Moreover, soil N variables were significantly correlated with soil OC, TN, and C:N ratio in the present study (Table 5), suggesting that soil N availability significantly increased with soil OC and TN accumulation following vegetation restoration. In consideration of the accumulation of OC and TN following vegetation restoration, SOM can provide a substantial amount of substrate for soil microbes to stimulate microbial activity (Li et al., 2018). Therefore, an increase in soil OC and TN may be responsible for the increase in net soil N transformation rates and inorganic N pools. A previous study in the karst region of Southwest China has reported that the correlation between soil NH_4^+–N concentration and N nitrification is weak during post-agricultural succession, but a significant positive correlation was found between NH_4^+–N and soil net mineralization (Song et al., 2019). The

Table 4
Correlation analyses for soil structure parameters and soil properties.

	MWD	MGD	Clay	Ca^{2+}	OC	Soil aggregates (mm)				
						5–10	2–5	1–2	0.25–1	< 0.25
MWD	1	0.997**	0.661*	0.596*	0.449	0.997**	−0.926**	−0.988**	−0.918**	−0.483
MGD		1	0.655*	0.579*	0.423	0.990**	−0.909**	−0.990**	−0.918**	−0.518
Clay			1	0.479	0.275	0.696**	−0.781**	−0.625*	−0.43	−0.482
Ca^{2+}				1	0.722**	0.630*	−0.712**	−0.596*	−0.307	−0.734**
OC					1	0.457	−0.453	−0.497	−0.278	−0.589*

MWD: mean weight diameter (mm); MGD: geometric mean diameter; clay: soil particle size < 0.001 mm (%); Ca^{2+}: exchangeable calcium ($mg\ g^{-1}$); OC: soil organic carbon ($g\ kg^{-1}$). ** and * indicates significance at $P < 0.01$ and at $P < 0.05$, respectively.

Table 5
Correlations among soil variables following vegetation restoration succession.

	OC	OCs	TN	TNs	C:N	Ca^{2+}	pH	NO_3^-–N	NH_4^+–N	NMR	NNR	NAR
OC												
OCs	0.982**											
TN	0.949**	0.899**										
TNs	0.957**	0.947**	0.977**									
C:N	0.702**	0.778**	0.444	0.537*								
Ca^{2+}	0.722**	0.709**	0.597*	0.597*	0.671*							
pH	0.641*	0.605*	0.483	0.446	0.670*	0.862**						
NO_3^-–N	0.811**	0.793**	0.682*	0.675*	0.723**	0.713**	0.791**					
NH_4^+–N	0.643*	0.644*	0.768**	0.807**	0.131	0.393	0.18	0.352				
NMR	0.906**	0.850**	0.938**	0.902**	0.447	0.514	0.514	0.798**	0.660*			
NNR	0.750**	0.727**	0.595*	0.574*	0.745**	0.624*	0.699**	0.921**	0.107	0.730**		
NAR	0.564*	0.506	0.767**	0.736**	−0.101	0.119	0.044	0.234	0.855**	0.722**	0.054	

OC, OC concentrations in total soil ($g\ kg^{-1}$) ($g\ kg^{-1}$); TN, TN concentrations in total soil ($g\ kg^{-1}$); OCs, OC stocks in total soil ($kg\ m^{-2}$); TNs, TN stocks in total soil ($g\ m^{-2}$); C:N, soil C:N ratios in total soil; Ca^{2+}: exchangeable calcium content in total soil ($mg\ g^{-1}$); NO_3^-–N, soil NO_3^-–N concentrations in total soil ($g\ kg^{-1}$); NH_4^+–N, soil NH_4^+–N concentrations in total soil ($g\ kg^{-1}$); NMR, soil net N mineralization rate ($mg\ kg^{-1}\ 28\ d^{-1}$); NNR, soil net N nitrification rate ($mg\ kg^{-1}\ 28\ d^{-1}$); NAR, soil net N ammonification rate ($mg\ kg^{-1}\ 28\ d^{-1}$). ** and * indicates significance at $P < 0.01$) and at $P < 0.05$, respectively.

same results were obtained in the present study (Table 5). Soil NH_4^+–N concentration showed a strong correlation with net N ammonification rate (Table 5). Therefore, net soil NMR and NAR can reflect NH_4^+ availability better than net soil NNR in the present study. In addition, significant positive correlations between soil exchangeable calcium content and soil NO_3^-–N and NNR (Table 5) were found, contributing to the strong correlation between soil exchangeable calcium and soil OC or TN. Another possible reason is that the addition of calcium can regulate soil pH and thus the composition and activity of a microbial community (Rousk et al., 2009). The reciprocal interactions between soil calcium content and the composition of species successively influence the quality of plant litter available for N mineralization (Page and Mitchell, 2008). In particular, the soil OC and TN levels in the farmland were comparable to those in grassland, but a higher NMR and NNR were noted in farmland compared with those in grassland (Fig. 2B). Similar results were found in other karst regions (Song et al., 2019). This result was obtained probably because the frequent tillage and application of fertilizers in farmlands disrupted soil aggregation, resulting in high mineralization and nitrification rates. Nevertheless, high mineralization and nitrification rates in farmlands can provide a sufficient supply of nitrogen for plant growth in the short term.

Soil N mineralization often drives soil N nitrification (Booth et al., 2005; Deng et al., 2014b) and ammonification (Table 5). Consequently, vegetation succession significantly increased soil NMR, NNR, and NAR and inorganic N pools (Fig. 2). The increases in soil N transformations and availability probably confirmed that soil N limitation occurred in the initial stages of vegetation restoration.

5. Conclusions

Our results demonstrated that abandoning farmlands for natural vegetation restoration significantly increased OC and TN stocks in whole soil and aggregates due to the accumulation of OC and TN in large soil aggregates (5–10 mm). Vegetation restoration significantly increased the proportion and stability of large aggregates (5–10 mm), which can physically protect OC and TN from mineralization. Soil C:N ratio and exchangeable calcium content are important factors associated with soil OC and TN sequestration. We found that soil OC and TN were significantly positively correlated in whole soil and aggregates, indicating that soil OC and TN were closely accumulated. However, the increases in soil C:N and NO_3^-–N: NH_4^+–N ratios implied that the increase in soil OC sequestration might be limited by soil N in the initial stages of vegetation restoration. Soil NMR and NNR and soil N availability significantly increased with soil OC and TN accumulation during vegetation restoration. This result probably confirmed that soil N limitation occurred in the initial stages of vegetation restoration.

Our results suggested that abandoning farmlands for natural vegetation restoration can improve the soil structure, facilitate the coupled accumulation of soil C and N, and enhance soil N transformation rates and N availability. Therefore, natural vegetation restoration can sustain soil OC sequestration in the long term in the karst rocky desertification regions of Southwest China. Soil C and N ecological processes and N availability can recover following the cessation of human disturbances.

Declaration of Competing Interest

The authors declared that they have no conflicts of interest to this work.

Acknowledgments

This study was supported by the National Natural Science Foundation of China (41601584), Guizhou Provincial Science and Technology Foundation (Qiankehe Foundation [2017]1417), the National Key Research and Development Program of China (2016YFC0502603), Earthquake science and Technology Spark Program, China Earthquake Administration (XH19028YSX), Guizhou Provincial Science and Technology Program (Qiankehe Platform Talent [2017]5726), Guizhou Normal University Doctoral Research Fund (No. 2014), and Domestic First-class Discipline Construction Project in Guizhou (Geography of Guizhou Normal University, Qiankehe Research Foundation [2017] 85). We are grateful for the help from the Prof. Daoxian Yuan of School of Geographical Sciences, Southwest University, Chongqing, China.

References

Benbi, D.K., Brar, K., Toor, A.S., Singh, P., 2015. Total and labile pools of soil organic carbon in cultivated and undisturbed soils in northern India. Geoderma. 237-238, 149–158.

Bhogal, A., Hatch, D.J., Shepherd, M.A., Jarvis, S.C., 1999. Comparison of methodologies for field measurement of net nitrogen mineralisation in arable soils. Plant Soil 207, 15–28.

Booth, M.S., Stark, J.M., Rastetter, E., 2005. Controls on nitrogen cycling in terrestrial ecosystems_ A synthetic analysis of literature data. Ecol. Monogr. 75, 139–157.

Deng, L., Liu, G.B., Shangguan, Z.P., 2014a. Land-use conversion and changing soil carbon stocks in China's 'Grain-for-Green' program: a synthesis. Glob. Chang. Biol. 20 (11), 3544–3556.

Deng, Q., Cheng, X., Yang, Y., Zhang, Q., Luo, Y., 2014b. Carbon–nitrogen interactions during afforestation in Central China. Soil Biol. Biochem. 69, 119–122.

Deng, L., Kim, D.-G., Peng, C., Shangguan, Z., 2018. Controls of soil and aggregate-associated organic carbon variations following natural vegetation restoration on the Loess Plateau in China. LDD. 29 (11), 3974–3984.

Ge, N., Wei, X., Wang, X., Liu, X., Shao, M., Jia, X., Li, X., Zhang, Q., 2019. Soil texture determines the distribution of aggregate-associated carbon, nitrogen and phosphorous under two contrasting land use types in the Loess Plateau. Catena. 172, 148–157.

Hu, N., Ma, Z., Lan, J., Wu, Y., Fu, W., Yuan, H., Lou, Y., 2016. Leaf litter decomposition characters and impact on soil orgainc carbon/nitrogen in different vegetation restorations of karst rocky desertification: a example of the Zhongliang Mountain in Chongqing. Carsologica Sin. 35 (5), 539–549.

Hu, P., Liu, S., Ye, Y., Zhang, W., He, X., Su, Y., Wang, K., 2018. Soil carbon and nitrogen accumulation following agricultural abandonment in a subtropical karst region. Appl. Soil Ecol. 132, 169–178.

ISSAS, 1978. Soil Physical and Chemical Analysis. Shanghai Science and Technology Press, Shanghai.

Jiang, Z., Lian, Y., Qin, X., 2014. Rocky desertification in Southwest China: Impacts, causes, and restoration. Earth-Sci. Rev. 132, 1–12.

Kaiser, M., Walter, K., Ellerbrock, R.H., Sommer, M., 2011. Effects of land use and mineral characteristics on the organic carbon content, and the amount and composition of Na-pyrophosphate-soluble organic matter, in subsurface soils. Eur. J. Soil Sci. 62 (2), 226–236.

Knops, J.M., Tilman, D., 2000. Dynamics of soil nitrogen and carbon accumulation for 61 years after agricultural abandonment. Ecology. 81, 88–98.

Kumar, S., Singh, A.K., Ghosh, P., 2018. Distribution of soil organic carbon and glomalin related soil protein in reclaimed coal mine-land chronosequence under tropical condition. Sci. Total Environ. 625, 1341–1350.

Laganière, J., Angers, D.A., Paré, D., 2010. Carbon accumulation in agricultural soils after afforestation: a meta-analysis. Glob. Chang. Biol. 16 (1), 439–453.

LeBauer, D.S., Treseder, K.K., 2008. Nitrogen limitation of net primary productivity in terrestrial ecosystems is globally distributed. Ecology. 89, 371–379.

Li, D., Niu, S., Luo, Y., 2012. Global patterns of the dynamics of soil carbon and nitrogen stocks following afforestation: a meta-analysis. New Phytol. 195 (1), 172–181.

Li, D., Wen, L., Yang, L., Luo, P., Xiao, K., Chen, H., Zhang, W., He, X., Chen, H., Wang, K., 2017. Dynamics of soil organic carbon and nitrogen following agricultural abandonment in a karst region. J. Geophys. Res. Biogeosci. 122 (1), 230–242.

Li, X., Yang, H., Shi, W., Li, Y., Guo, Q., 2018. Afforestation with xerophytic shrubs accelerates soil net nitrogen nitrification and mineralization in the Tengger Desert, Northern China. Catena. 169, 11–20.

Liu, J., Shen, L., Wang, Z., Duan, S., Wu, W., Peng, X., Wu, C., Jiang, Y., 2019a. Response of plants water uptake patterns to tunnels excavation based on stable isotopes in a karst trough valley. JHyd. 571, 485–493.

Liu, X., Zhang, W., Wu, M., Ye, Y., Wang, K., Li, D., 2019b. Changes in soil nitrogen stocks following vegetation restoration in a typical karst catchment. LDD. 30 (1), 60–72.

Lu, R., 2000. Soil Argrochemistry Analysis Protocoes. China Agriculture Science Press, Beijing.

Miller, A.J., Amundson, R., Burke, I.C., Yonker, C., 2004. The effect of climate and cultivation on soil organic C and N. Biogeochemistry. 67, 57–72.

Page, B.D., Mitchell, M.J., 2008. Influences of a calcium gradient on soil inorganic nitrogen in the Adirondack Mountains, New York. Ecol. Appl. 18, 1604–1614. https://doi.org/10.1890/07-0150.1.

Post, W.M., Pastor, J., Zinke, P.J., Stangenberger, A.G., 1985. Global patterns of soil nitrogen storage. Nature. 317, 613–616.

Qiu, L., Wei, X., Ma, T., Wei, Y., Horton, R., Zhang, X., Cheng, J., 2015. Effects of land-use change on soil organic carbon and nitrogen. Plant Soil 390, 419–430.

Rousk, J., Brookes, P.C., Baath, E., 2009. Contrasting soil pH effects on fungal and bacterial growth suggest functional redundancy in carbon mineralization. Appl. Environ. Microbiol. 75 (6), 1589–1596.

Schlüter, S., Sammartino, S., Koestel, J., 2020. Exploring the relationship between soil structure and soil functions via pore-scale imaging. Geoderma. 370, 114370.

Singh, A.K., Rai, A., Singh, N., 2016. Effect of long term land use systems on fractions of glomalin and soil organic carbon in the Indo-Gangetic plain. Geoderma. 277, 41–50.

Six, J., Paustian, K., 2014. Aggregate-associated soil organic matter as an ecosystem property and a measurement tool. Soil Biol. Biochem. 68, A4–A9.

Six, J., Conant, R.T., Paul, E.A., Paustian, K., 2002. Stabilization mechanisms of soil organic matter: Implications for C-saturation of soils. Plant Soil 241, 155–176.

Six, J., Bossuyt, H., Degryze, S., Denef, K., 2004. A history of research on the link between (micro)aggregates, soil biota, and soil organic matter dynamics. Soil Tillage Res. 79 (1), 7–31.

Song, M., He, T., Chen, H., Wang, K., Li, D., 2019. Dynamics of soil gross nitrogen transformations during post-agricultural succession in a subtropical karst region. Geoderma. 341, 1–9.

Tang, F.K., Cui, M., Lu, Q., Liu, Y.G., Guo, H.Y., Zhou, J.X., 2016. Effects of vegetation restoration on the aggregate stability and distribution of aggregate-associated organic carbon in a typical karst gorge region. Solid Earth. 7 (1), 141–151.

Tisdall, J.M., Oades, J.M., 1982. Organic matter and water-stable aggregates in soils. Eur. J. Soil Sci. 33 (2), 141–163.

Tong, X., Brandt, M., Yue, Y., Horion, S., Wang, K., Keersmaecker, W.D., Tian, F., Schurgers, G., Xiao, X., Luo, Y., Chen, C., Myneni, R., Shi, Z., Chen, H., Fensholt, R., 2018. Increased vegetation growth and carbon stock in China karst via ecological engineering. Nat. Sustain. 1 (1), 44–50.

von Lützow, M., Kögel-Knabner, I., Ekschmitt, K., Matzner, E., Guggenberger, G., Marschner, B., Flessa, H., 2006. Stabilization of organic matter in temperate soils: mechanisms and their relevance under different soil conditions - a review. Eur. J. Soil Sci. 57 (4), 426–445.

Wang, Y., Ran, L., Fang, N., Shi, Z., 2018. Aggregate stability and associated organic carbon and nitrogen as affected by soil erosion and vegetation rehabilitation on the Loess Plateau. Catena. 167, 257–265.

Wang, K., Zhang, C., Chen, H., Yue, Y., Zhang, W., Zhang, M., Qi, X., Fu, Z., 2019. Karst landscapes of China: patterns, ecosystem processes and services. Landsc. Ecol. 34 (12), 2743–2763.

Wei, X., Li, X., Jia, X., Shao, M., 2012. Accumulation of soil organic carbon in aggregates after afforestation on abandoned farmland. Biol. Fertil. Soils 49 (6), 637–646.

Wen, L., Li, D., Yang, L., Luo, P., Chen, H., Xiao, K., Song, T., Zhang, W., He, X., Chen, H., Wang, K., 2016. Rapid recuperation of soil nitrogen following agricultural abandonment in a karst area, Southwest China. Biogeochemistry. 129 (3), 341–354.

Wu, Q., Jiang, X., Lu, Q., Li, J., Chen, J., 2020. Changes in soil organic carbon and aggregate stability following a chronosequence of Liriodendron chinense plantations. J. For. Res. https://doi.org/10.1007/s11676-020-01110-0. https://link.springer.com/article/10.1007/s11676-020-01110-0.

Xiao, K., He, T., Chen, H., Peng, W., Song, T., Wang, K., Li, D., 2017a. Impacts of vegetation restoration strategies on soil organic carbon and nitrogen dynamics in a karst area, Southwest China. Ecol. Eng. 101, 247–254.

Xiao, S., Zhang, W., Ye, Y., Zhao, J., Wang, K., 2017b. Soil aggregate mediates the impacts of land uses on organic carbon, total nitrogen, and microbial activity in a Karst ecosystem. Sci. Rep. 7, 41402.

Xiao, K., Li, D., Wen, L., Yang, L., Luo, P., Chen, H., Wang, K., 2018. Dynamics of soil nitrogen availability during post-agricultural succession in a karst region, Southwest China. Geoderma. 314, 184–189.

Yang, L., Luo, P., Wen, L., Li, D., 2016. Soil organic carbon accumulation during post-agricultural succession in a karst area, Southwest China. Sci. Rep. 6, 37118.

Yang, J., Xu, X., Liu, M., Xu, C., Zhang, Y., Luo, W., Zhang, R., Li, X., Kiely, G., Wang, K., 2017. Effects of "grain for Green" program on soil hydrologic functions in karst landscapes, southwestern China. Agric. Ecosyst. Environ. 247, 120–129.

Yao, S., Qin, J., Peng, X., Zhang, B., 2009. The effects of vegetation on restoration of physical stability of a severely degraded soil in China. Ecol. Eng. 35 (5), 723–734.

Zhang, W., Zhao, J., Pan, F., Li, D., Chen, H., Wang, K., 2015. Changes in nitrogen and phosphorus limitation during secondary succession in a karst region in Southwest China. Plant Soil 391, 77–91.

Zhang, P., Zhang, Y., Jia, J., Cui, Y., Wang, X., Zhang, Y., Zhang, X., Wang, Y., 2019a. Soil aggregation and aggregate-associated organic C and total N as affected by revegetation pattern at a surface mine on the Loess Plateau, China. SSSAJ. 83 (2), 388.

Zhang, Y., Xu, X., Li, Z., Liu, M., Xu, C., Zhang, R., Luo, W., 2019b. Effects of vegetation restoration on soil quality in degraded karst landscapes of Southwest China. Sci. Total Environ. 650 (Pt 2), 2657–2665.

Zhong, Z., Han, X., Xu, Y., Zhang, W., Fu, S., Liu, W., Ren, C., Yang, G., Ren, G., 2019. Effects of land use change on organic carbon dynamics associated with soil aggregate fractions on the Loess Plateau, China. LDD. 30 (9), 1070–1082.

Zhu, G., Shangguan, Z., Deng, L., 2017. Soil aggregate stability and aggregate-associated carbon and nitrogen in natural restoration grassland and Chinese red pine plantation on the Loess Plateau. Catena. 149, 253–260.